

Two-parameter bifurcation curves in power electronic converters¹

E. Fossas[†], S. J. Hogan[§] and T. M. Seara[‡]

26th July 2006

[†]*Institute of Industrial and Control Engineering, Universitat Politècnica de Catalunya, Av. Diagonal 647, 08028 Barcelona, Spain*

[§]*Department of Engineering Mathematics, Queen's Building, University Walk, Bristol BS8 1TR, England*

[‡]*Department of Applied Mathematics I, Universitat Politècnica de Catalunya, Av. Diagonal 647, 08028 Barcelona, Spain*

Abstract

In many control problems, the control strategy is phrased in terms of average quantities. In this paper we prove the general result that, given a linear system $\dot{x} = Ax + u$ where A is hyperbolic, u is piecewise linear and L -periodic, such that $\int_0^L u(t)dt = 0$, then there exists a unique L -periodic solution $x = x_p(t)$ such that $\int_0^L x_p(t)dt = 0$. We then consider a DC/DC buck (step-down) converter controlled by the ZAD (zero-average dynamics) strategy. The ZAD strategy sets the *duty cycle*, d (the length of time the input voltage is applied across an inductance), by ensuring that, on average, a function of the state variables is always zero. The two control parameters are v_{ref} , a reference voltage that the circuit is required to follow, and k_s , a time constant which controls the approach to the zero average. We show how to calculate d exactly for a periodic system response, without knowledge of the state space solutions. In particular we show that for a T -periodic response d is *independent* of k_s . We calculate curves in (v_{ref}, k_s) space at which a T -periodic response of the system undergoes period doubling and corner collision bifurcations, the latter occurring when the duty cycle saturates and is unable to switch. We also show the presence of a codimension two bifurcation in this system when a corner collision bifurcation and a saddle node bifurcation collide, to produce stable unsaturated $2T$ -periodic responses which can be obtained either in the presence or absence of the stable T -periodic response.

¹Abbreviated Title: Bifurcations in power electronic converters

1 Introduction

Electronic devices such as mobile phones and laptop computers contain circuits that require differing voltage levels. These voltages, which can be higher or lower than that of the supply, have to be stable over a wide range of operating conditions, including variable ambient temperature and decreasing input voltage as battery power reduces between charges. Such a conversion is not easy to achieve with a simple circuit (in particular it is impossible to achieve a higher voltage with voltage or linear regulators). Instead, voltage is changed by switched mode conversion in a circuit known as a power electronic converter. The basic idea is that the input voltage is applied across an inductance, allowing for the build up of magnetic energy. The voltage is then switched and the stored energy transferred, in a controlled way, to the output voltage. This switching cycle, usually governed by an external clock, is very short (typically in the order of 1MHz) and, in more sophisticated converters, the time that the voltage is applied to the inductance (the *duty cycle*) is allowed to vary, in order to produce the desired system behaviour. Depending on what voltage is required, different converters have different designs (and different names). A full account of power electronic converter is given in Mohan *et al.* (2002).

With the rapid pace of development of electronic devices, there is demand for stable voltage conversion that is available over a wide range of system parameters. In addition the output of power electronic converters can be chaotic (Fossas & Olivar 1996, Yuan *et al.* 1998), with the voltage varying considerably between switching cycles. Therefore some form of control strategy must be introduced in order to extend the operating range of power electronic converters whilst, at the same time, avoiding unpredictable (and hence undesirable) behaviour.

Banerjee and Verghese (2001) give a detailed account of the modelling of power electronic converters by ordinary differential equations with a discontinuous right-hand side (often termed Filippov systems). These equations are usually linear in the system dependent variables (state variables) of voltage and current, with the discontinuity occurring because of the switching control action, which is a nonlinear function of the state variables. For many years the linear nature of these equations meant that such systems were dismissed as being of little interest mathematically. But now they are known to contain not only behaviour typical of nonlinear smooth systems (such as period doubling bifurcations and chaos) but also dynamics that is unique (such as period adding and corner collision bifurcations). Di Bernardo *et al.* (2006) give a comprehensive account of the latest developments in this field.

In this paper, we shall study the example of the DC/DC buck (step-down) converter controlled by the ZAD (zero-average dynamics) strategy (Biel, Fossas & Griño, 2001). A recent two parameter study of this problem by Angulo *et al.* (2005) appeared to show in this problem the presence of a previously unknown type of nonsmooth bifurcation. This bifurcation occurred as a period-doubling bifurcation collided *tangentially* with a corner collision bifurcation, as the whole system saturated (the control strategy does not switch to the duty

cycle in any clock cycle). That study, which was inconclusive, was entirely numerical and used an approximation to the ZAD strategy that allowed for efficient implementation.

We carry out an exact analysis of the problem, using the full systems equations with no approximations. In §2 we introduce the DC/DC buck converter with ZAD strategy, including the two different coordinate representations that we shall use in this paper. Then in §3, we prove a result which allows us to calculate exactly the duty cycle d of a periodic system response, in the absence of detailed knowledge of the dynamics of the problem. In §4, we analytically calculate the period doubling bifurcation curve of a T -periodic system solution in (v_{ref}, k_s) parameter space. We perform a similar calculation in §5, where we analytically calculate the corner collision bifurcation curve in (v_{ref}, k_s) space where the $2T$ -periodic solution saturates (that is, when one duty cycle of the response equals 0 or 1) and give exact results for points on the curve in the limiting cases $v_{ref} = \pm 1$. In §6 we confirm and extend the results of Angulo *et al.* (2005), by showing that the period doubling bifurcation curve and the corner collision bifurcation curve intersect tangentially, normal to and at the line $v_{ref} = 1$ and tangentially at the line $v_{ref} = -1$. We also note in this section a codimension two bifurcation point where the corner collision curve collides with a saddle node bifurcation and we detect numerically this intersection for some specific parameter values. Finally in §7, we provide three different codimension one bifurcation diagrams that occur in this system as the duty cycle, d , varies with k_s for fixed v_{ref} .

2 The DC/DC buck converter with ZAD strategy

The buck converter circuit switches between two distinct linear topologies depending on the value of a control input. The control action considered here, zero average dynamics (ZAD), was proposed in Fossas *et al.* (2001) and Ramos *et al.* (2003). It involves the direct design of the duty cycle and is implemented in a single updated centred pulse width modulation (PWM). Figure 1 depicts the block diagram of the converter. The signal reference v_{ref} corresponds to the required output voltage which, in this paper, we shall take to be constant in time. The control input u takes discrete, constant, values in the set $\{B_1, B_2\}$. In this paper, we shall restrict attention to the case $B_2 = -B_1$, to simplify the analysis. The voltage v on the capacitor and the current i on the inductor are the dependent (state) variables. We apply the following non-dimensionalisation: $x_1 = v/E$, $x_2 = \frac{1}{E}\sqrt{\frac{L}{C}}i$, $t = \tau/\sqrt{LC}$ and define parameters $\gamma = \frac{1}{R}\sqrt{\frac{L}{C}}$ and $T = T_c/\sqrt{LC}$. Parameter values are chosen as $R = 20\Omega$, $C = 40\mu F$, $L = 2mH$, $E = 40V$. The clock cycle (sampling period) is $T_c = 50\mu s$, hence $\gamma = 0.35$ and $T = 0.1767$.

Then the equations of the DC/DC buck converter in dimensionless form can

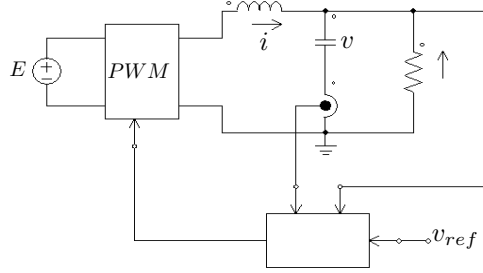


Figure 1: Circuit of a PWM-controlled power converter.

be written as

$$\dot{x} = Ax + u \quad (1)$$

where $x = (x_1, x_2)$, u is given by

$$u = \begin{cases} B_1, & kT \leq t < kT + Td_k/2 \\ B_2, & kT + Td_k/2 \leq t < (k+1)T - Td_k/2 \\ B_1, & (k+1)T - Td_k/2 \leq t < (k+1)T \end{cases} \quad (2)$$

where d_k is the (scaled) duty cycle and

$$A = \begin{pmatrix} -\gamma & 1 \\ -1 & 0 \end{pmatrix}, \quad B_1 = \begin{pmatrix} 0 \\ 1 \end{pmatrix}, \quad B_2 = -B_1 = \begin{pmatrix} 0 \\ -1 \end{pmatrix} \quad (3)$$

Note that $d_k \in [0, 1]$ and that $d_k = 0$ corresponds to $u = B_2$ and $d_k = 1$ corresponds to $u = B_1$ on $[kT, (k+1)T]$.

In (2), the duty cycle d_k of the pulse width modulation is determined by ensuring that the average of some function, s , of the state variables $x = (x_1, x_2)$, taken over the sampling period T , equals zero. This will also guarantee that the output x_1 follows the reference v_{ref} .

As in Bilalovic *et al.* (1983), Venkataraman *et al.* (1985) and Carpita *et al.* (1988), we define

$$s(t) \equiv (x_1(t) - v_{ref}) + k_s(\dot{x}_1(t) - \dot{v}_{ref}) \quad (4)$$

where k_s is a time constant, associated with first order dynamics on the error surface $s = 0$. Note that our choice of a constant reference output voltage v_{ref} means that the definition of s simplifies to

$$s(t) \equiv (x_1(t) - v_{ref}) + k_s \dot{x}_1(t) \quad (5)$$

and it is this that we shall use in the remainder of the paper. The zero average dynamics (ZAD) strategy is then to choose d_k such that

$$\int_{kT}^{(k+1)T} s(t) dt = 0. \quad (6)$$

We can recast the problem in a different form, which will be useful subsequently. Following Angulo, Fossas & Seara (2005), we set

$$e(t) = x_1(t) - v_{ref} \quad (7)$$

and hence from (5) the ZAD function becomes

$$s(t) = e(t) + k_s \dot{e}(t) \quad (8)$$

Transforming to coordinates $x = (e, s)$ the dynamics are still governed by (1), (2), (5) and (6) but now (3) becomes

$$A = \begin{pmatrix} -1/k_s & 1/k_s \\ \gamma - 1/k_s - k_s & 1/k_s - \gamma \end{pmatrix}, \quad B_1 = \begin{pmatrix} 0 \\ (1 - v_{ref})k_s \end{pmatrix}, \quad B_2 = \begin{pmatrix} 0 \\ (-1 - v_{ref})k_s \end{pmatrix} \quad (9)$$

3 Periodic orbits in zero average dynamics

Before embarking on a detailed study of the dynamics of the system described in the last section, we will prove a very useful result which we shall use many times in this paper.

Lemma 3.1. *Given a linear system*

$$\dot{x} = Ax + u \quad (10)$$

where A is hyperbolic, u is piecewise linear and L -periodic, such that $\int_0^L u(t)dt = 0$, then there exists a unique L -periodic solution $x = x_p(t)$ such that $\int_0^L x_p(t)dt = 0$

Proof. Define $y = x - U$ where $U(t) \equiv \int_0^t u(\tau)d\tau$. Then U is everywhere continuous, L -periodic and differentiable except at points where u is discontinuous. It is straightforward to show that if x is a continuous solution of system (10), y is everywhere differentiable and satisfies $\dot{y} = Ay + AU$, a linear system in y with a continuous periodic forced term. Thus, being A a hyperbolic matrix, there exists an unique L -periodic solution y_p . By periodicity, $\int_0^L \dot{y}_p dt = 0$ and hence

$$0 = \int_0^L \dot{y}_p dt = A \int_0^L (y_p + U) dt \quad (11)$$

Then $x_p = y_p + U$ is the unique L -periodic solution of (10). Since A is invertible we must have

$$\int_0^L x_p dt = \int_0^L (y_p + U) dt = 0 \quad (12)$$

which completes the proof. \square

It is straightforward to generalize this result to any piecewise continuous periodic function u with jump discontinuities having zero average. In Lemma 3.1 we adapt the general result to the case needed in this paper. At first glance, this result appears to be of little interest. In fact it allows us to calculate explicitly the duty cycle, d_k , of any periodic solution to the equations in the previous section, without having to find the solution itself.

If we take the control action u in the form given by equation (2), with B_1 and B_2 as in (9), a simple calculation shows that, taking

$$d_k = d = \frac{1 + v_{ref}}{2} \quad \forall k, \quad (13)$$

u is T -periodic and $\int_0^T u dt = 0$ as well. But lemma 3.1 implies that $\int_0^T x_p dt = 0$. So if we work in the transformed variables (e, s) , this implies that both $\int_0^T e_p dt = 0$ and $\int_0^T s_p dt = 0$. But the latter condition is just the ZAD control strategy. Thus for every T -periodic solution of the DC/DC buck converter problem, we have $d = \frac{1+v_{ref}}{2}$, independent of the exact form of the solution and, more importantly, *independent of the time constant k_s* . Note that in Angulo, Fossas & Seara (2005), (13) was used as an approximation to the duty cycle, under the assumption that $s(t)$ is approximately piecewise linear. In fact it is an exact result.

Since $d \in [0, 1]$, (13) implies that $v_{ref} \in [-1, 1]$. Since $x_1 = v/E$ follows the ZAD strategy, this implies that $v \in [-E, E]$, precisely the operating range of a buck converter.

Finally in this section, we derive the exact form of the initial conditions that give a T -periodic solution for the DC/DC buck converter with the ZAD control strategy.

Lemma 3.2. *Given the linear system (1), where matrix A and the function u are given by (2), (3) and $d_k = d$, the unique T -periodic solution has initial conditions*

$$x_0^* = -A^{-1}B_1 + 2(I - e^{AT})^{-1} \left(e^{A\frac{Td}{2}} - e^{AT(1-\frac{d}{2})} \right) A^{-1}B_1 \quad (14)$$

In addition, when $d = \frac{1+v_{ref}}{2}$, this periodic solution satisfies the ZAD strategy.

Proof. The general solution to the equation $\dot{x} = Ax + B$ with initial condition $x(0) = x_0$ and a constant forced vector B is just $x(t) = (-I + e^{At})A^{-1}B + e^{At}x_0$. Its repeated, consistent, use in the three sections of the control action (2) gives the result (14). \square

4 Period doubling

In this section, we find analytic conditions under which the unique T -periodic solution for the DC/DC buck converter with ZAD control strategy undergoes a (classical) period doubling bifurcation. The Poincaré map P , over a sampling

period $[kT, (k+1)T]$ is given in terms of the initial conditions x_0 and the duty cycle $d_k = d_k(x_0)$ by

$$P(x_0) = \phi(T, x_0, d_k) = e^{AT}x_0 + (e^{AT} - I)A^{-1}B_1 + 2 \left(e^{A\frac{Td_k}{2}} - e^{AT(1-\frac{d_k}{2})} \right) A^{-1}B_1 \quad (15)$$

where $\phi(t, x, d_k)$ denotes the flow of the differential equations (1).

The integral of the flow in terms of x and d_k is given by

$$\int_{kT}^{(k+1)T} \phi(t, x, d_k) dt = A^{-1} \left\{ (e^{AT} - I)(x + A^{-1}B_1) + 2 \left(e^{A\frac{Td_k}{2}} - e^{AT(1-\frac{d_k}{2})} \right) A^{-1}B_1 + T(1 - 2d_k)B_1 \right\} \quad (16)$$

Using (15) the Jacobian of the Poincaré map, $DP(x_0)$, is given by

$$DP(x_0) = e^{AT} + T \left(e^{A\frac{Td_k}{2}} + e^{AT(1-\frac{d_k}{2})} \right) B_1 \cdot \frac{\partial d_k}{\partial x_0} \quad (17)$$

The derivative of the duty cycle with respect to the initial conditions, $\frac{\partial d_k}{\partial x_0}$, can be obtained implicitly from the equation for the ZAD strategy, given by

$$\int_{kT}^{(k+1)T} s(t) dt = (1 - k_s \gamma, k_s) \cdot \int_{kT}^{(k+1)T} \phi(t, x, d_k) dt - v_{ref} T = 0 \quad (18)$$

When evaluating $\frac{\partial d_k}{\partial x_0}$ at $x = x_0^*$ given in (14), we use the result that $d_k = d = \frac{1+v_{ref}}{2}$.

A necessary condition for the periodic orbit to have a period doubling bifurcation is that one of the eigenvalues of the Jacobian of the Poincaré map equals minus one. So the period doubling bifurcation curve in the (v_{ref}, k_s) plane is given by

$$m_{pd}(v_{ref}, k_s) \equiv \det(DP(x_0^*) + I) = 0 \quad (19)$$

It is easy to check numerically that, if $(\bar{v}_{ref}, \bar{k}_s)$ belong to this curve, the periodic orbit is unstable for (\bar{v}_{ref}, k_s) , with $k_s < \bar{k}_s$, in other words, that the period doubling bifurcation is *subcritical*.

It is possible to obtain an analytical expression for this curve, but it is very cumbersome. Two points are of particular interest, namely the intersections of the curve with the lines $v_{ref} = \pm 1$. Thus, we define k_{s+}^* and k_{s-}^* such that

$$\begin{aligned} m_{pd}(1, k_{s+}^*) &= 0 \\ m_{pd}(-1, k_{s-}^*) &= 0 \end{aligned}$$

In next section, we give the exact expressions for these two points, which will be very useful for checking numerical calculations. It can also be shown that $\frac{\partial m_{pd}}{\partial v_{ref}}(1, k_{s+}^*) = 0$, so that the curve $m_{pd}(v_{ref}, k_s)$ intersects the line $v_{ref} = 1$ with vertical slope. Note that for $T = 0.1767$, $\gamma = 0.35$ we have that $k_{s+}^* = 2.8478517$ and $k_{s-}^* = 2.8497016$.

5 Nonsmooth bifurcation

After the period doubling bifurcation occurs ($k_s > \bar{k}_s$), the T -periodic orbit stabilizes and we have a (unstable) period two solution of the system, with duty cycles (d_1, d_2) , with (say) $d_1 > \frac{1+v_{ref}}{2}$ and $d_2 < \frac{1+v_{ref}}{2}$. But since $\frac{1+v_{ref}}{2} \in [0, 1]$, it is possible that one of these two duty cycles will saturate as k_s increases. In this section we construct curves in parameter space when this period two solution saturates, that is, d_1 becomes 1 or d_2 becomes 0.

If we look for a $(1, d)$ solution of system (1), we have to consider the $2T$ -periodic function

$$u = \begin{cases} B_1, & 0 \leq t < T + Td/2 \\ B_2, & T + Td/2 \leq t < 2T - Td/2 \\ B_1, & 2T - Td/2 \leq t < 2T \end{cases} \quad (20)$$

with B_1, B_2 given in (9).

We want the solution to satisfy the ZAD strategy in both periods. So we use lemma 3.1 with $L = 2T$. Since $\int_0^{2T} u dt = 0$, we have from (20) that

$$d = v_{ref} \quad (21)$$

which replaces (13) in what follows. Then, lemma 3.1 implies the existence of a $2T$ -periodic solution (e^{**}, s^{**}) verifying $\int_0^{2T} e^{**} = \int_0^{2T} s^{**} = 0$.

Note that $d \in [0, 1]$ only for positive v_{ref} . Hence, there exist $(1, d)$ periodic solutions in this case only. Proceeding analogously, it can be proved that $(d, 0)$ periodic solutions have $d = 1 + v_{ref}$. Thus, $d \in [0, 1]$ for negative v_{ref} only.

Going back to the original variables (x_1, x_2) we obtain

Lemma 5.1. *Given the linear system (1), where matrix A and the $2T$ -periodic function u are given by (3) and (20), the unique $2T$ -periodic solution has initial conditions*

$$x_0^{**} = -A^{-1}B_1 + 2(I - e^{2AT})^{-1} \left(e^{ATd/2} - e^{AT(1-d/2)} \right) A^{-1}B_1 \quad (22)$$

In addition, when $d = v_{ref}$, this periodic solution satisfies $\int_0^{2T} s^{**}(t) dt = 0$.

We know that $\int_0^{2T} s^{**}(t) dt = 0$ and so we complete the ZAD strategy if

$$m_{cc}(v_{ref}, k_s) \equiv \int_0^T s^{**}(t) dt = (1 - k_s \gamma, k_s) \cdot \int_0^T \phi(t, x_0^{**}, 1) dt - v_{ref} T = 0 \quad (23)$$

This equation defines the non-smooth bifurcation curve in (v_{ref}, k_s) parameter space. From (22), (16) and $d = v_{ref}$, it is straightforward to show that

$$\int_0^T \phi(t, x_0^{**}, 1) dt = A^{-1} \left\{ -2(I + e^{AT})^{-1} (e^{Av_{ref}T/2} - e^{AT(1-v_{ref}/2)}) A^{-1}B_1 - B_1 T \right\} \quad (24)$$

and hence that

$$\begin{aligned}
m_{cc}(v_{ref}, k_s) &= (1 - \gamma k_s, k_s) \cdot \\
&A^{-1} \left\{ -2(I + e^{AT})^{-1} (e^{Av_{ref}T/2} - e^{AT(1-v_{ref}/2)}) A^{-1} B_1 - B_1 T \right\} - v_{ref} T \\
&= (1 - \gamma k_s, k_s) \cdot \left\{ -2(\cosh \frac{AT}{2})^{-1} \sinh \frac{AT(v_{ref}-1)}{2} A^{-2} B_1 \right\} - (v_{ref} - 1) T
\end{aligned} \tag{25}$$

We know that A , B_1 and B_2 as given in (3) are independent of (k_s, v_{ref}) . So, from equation (25), it is straightforward that the curve $m_{cc}(v_{ref}, k_s)$ is linear in k_s and odd in v_{ref} , so that it can be written as

$$m_{cc}(v_{ref}, k_s) = (v_{ref} - 1) G_{cc}(v_{ref}, k_s) \tag{26}$$

where G_{cc} is linear in k_s and is even in $(v_{ref} - 1)$.

Moreover, a direct calculation shows that $G_{cc}(1, k_{s+}^*) = 0$, where

$$k_{s+}^* = \frac{\gamma}{2} - \alpha \frac{(\sinh \frac{\gamma T}{4})^2 + (\cos \frac{\alpha T}{2})^2 - \cosh \frac{\gamma T}{4} \cos \frac{\alpha T}{2}}{\sinh \frac{\gamma T}{4} \sin \frac{\alpha T}{2}} \tag{27}$$

and $\alpha = \sqrt{1 - (\frac{\gamma}{2})^2}$.

Summarizing, both the period doubling bifurcation curve and the nonsmooth bifurcation curve intersect the line $v_{ref} = 1$ at the same point where both curves are vertical in (v_{ref}, k_s) parameter space.

There are analogous results for $v_{ref} < 0$, when $d = 1 + v_{ref}$. Namely, that $m_{cc}(v_{ref}, k_s) = (v_{ref} + 1) \hat{G}_{cc}(v_{ref}, k_s)$ is linear in k_s . Moreover $\hat{G}_{cc}(-1, k_{s-}^*) = 0$, where k_{s-}^* is given by:

$$k_{s-}^* = \frac{2 \sin \alpha T}{\gamma \sin \alpha T + 2\alpha \sinh \frac{\gamma T}{2}} \tag{28}$$

In this case, both the period doubling bifurcation curve and the nonsmooth bifurcation curve intersect the line $v_{ref} = -1$ also at the same point, but non-vertically.

6 Two parameter bifurcation diagram

In this section, we plot in (v_{ref}, k_s) parameter space, the period doubling bifurcation curve, given by equation (19), together with the corner collision curve, equation (25) for $v_{ref} > 0$ and its equivalent for $v_{ref} < 0$. The results are shown in figure 2. The period doubling curve is given by AEF , the corner collision curve in $v_{ref} > 0$ by AD and in $v_{ref} < 0$ by DF . Note the very narrow horizontal scale. We shall now discuss each of the 6 labelled points individually.

6.1 Point A

This is the point $(1, k_{s+}^*)$, where k_{s+}^* is given in (27). The two curves are tangent at this point and intersect the line $v_{ref} = 1$ normally, thus confirming the work

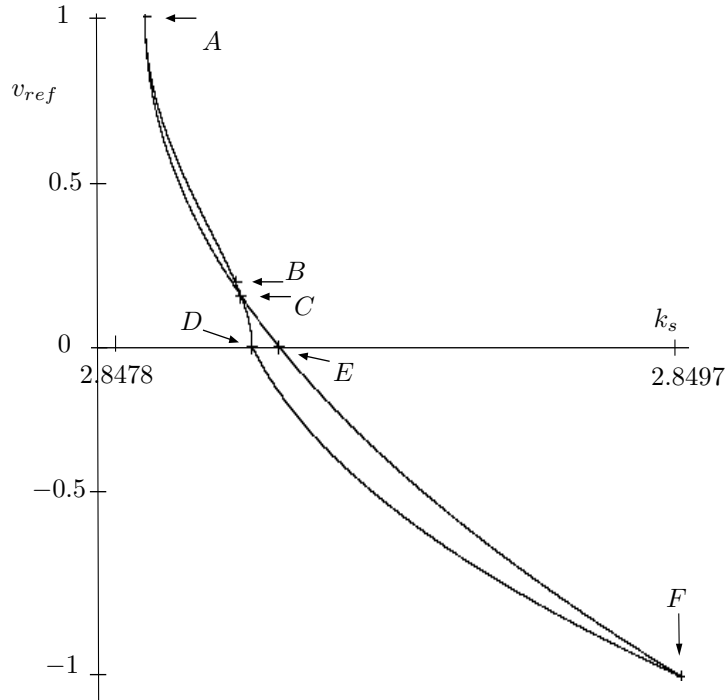


Figure 2: Period doubling and corner collision curves in (v_{ref}, k_s) parameter space. The labelled points are explained in the text.

of Angulo *et al.* (2005). That work used a piecewise linear approximation to the ZAD function s , which resulted in both a different value for k_{s+}^* , and different behaviour of the curves for $v_{ref} < 1$. The curves in figure 2 were all calculated analytically using *MAPLE* with 200 digits accuracy. Physically at this point, the circuit is not switching at all, but stays saturated with $d = 1$ and $u = B_1$. We speculate that all smooth and nonsmooth bifurcation curves pass through this point.

6.2 Point B

For $T = 0.1767$, $\gamma = 0.35$ there is a point $(\tilde{v}_{ref}, \tilde{k}_s)$, with $\tilde{v}_{ref} = 0.1943187$ and $\tilde{k}_s = 2.8481633$ which belongs to the corner collision curve, where the saturated $2T$ -periodic orbit experiences a saddle node bifurcation, that is, where $DP^2(x_0^{**})$ has an eigenvalue equal to one (x_0^{**} are the initial conditions of the $2T$ -periodic orbit given in lemma 5.1). This is a codimension-2 nonsmooth bifurcation point (see Kowalczyk *et al.* (2006) for a discussion of such points). A line of saddle node bifurcations (not shown) then emanates from B for $k_s > \tilde{k}_s$.

6.3 Point C

The curves $m_{cc}(v_{ref}, k_s)$ and $m_{pd}(v_{ref}, k_s)$ cross at $(\check{v}_{ref}, \check{k}_s)$, with $\check{v}_{ref} = 0.1549348$, $\check{k}_s = 2.8481818$ when $T = 0.1767$, $\gamma = 0.35$. However there is no exchange of stability here, since the curves relate to different solutions.

6.4 Points D,E

D is simply the point where, at $v_{ref} = 0$, the two separate corner collision curves meet. They do so continuously but not differentiably. In contrast at E , also on $v_{ref} = 0$, the period doubling bifurcation curve is smooth.

6.5 Point F

This is the point $(-1, k_{s-}^*)$, where k_{s-}^* is given in (28). The two curves are tangent at this point, but do not intersect the line $v_{ref} = -1$ normally, in contrast to the behaviour at $v_{ref} = 1$. The circuit is not switching at all, staying saturated with $d = 0$ and $u = B_2$. As with point A , we speculate that all smooth and nonsmooth bifurcation curves pass through this point.

7 One parameter bifurcation diagrams

There are three different types of behaviour in figure 2, for fixed v_{ref} , as k_s is varied. For $v_{ref} \in (A, B)$, the period doubling bifurcation occurs before the corner collision bifurcation. The upper (unstable) branch of the $2T$ -periodic solution saturates at the corner collision to produce an unstable solution with $d = 1$ in one period, the other branch has $d = v_{ref}$ since $v_{ref} > 0$. This behaviour is sketched in figure 3.

For $v_{ref} \in (B, C)$, as k_s is varied, the period doubling is still before the corner collision bifurcation, which is then followed by a saddle node bifurcation. Following the (unstable) branches of the $2T$ -periodic solution, both stabilize via a saddle node bifurcation to produce a stable *unsaturated* solution which subsequently undergoes a corner collision bifurcation to produce a stable *saturated* $2T$ -periodic solution, with duty cycles $(1, v_{ref})$. In this case we were able to find two coexisting stable solutions between the corner collision and the saddle node bifurcations, one saturated and the other unsaturated. So for $v_{ref} = 0.175$ and $k_s = 2.8483$ we found an unsaturated stable $2T$ -periodic solution with $d_1 = 0.75608$ and $d_2 = 0.0.41891$ (with eigenvalues 0.883372, 0.999998). This is illustrated in figure 4.

Finally for $v_{ref} \in (C, F)$, the order of the bifurcations for increasing k_s is now changed. Following the unstable branches of the period doubled solution, we find that they first undergo a saddle node bifurcation which then undergoes a corner collision bifurcation at a value of k_s *smaller* than that of the period doubling. This is illustrated in figure 5. Therefore there is a range of k_s in which an unsaturated $2T$ -periodic solution is stable when the T -periodic solution is unstable. For $v_{ref} = 0.01$, the corner collision occurs at $k_s = 2.8482212$ and

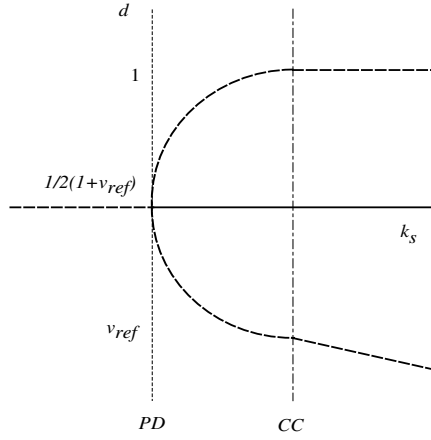


Figure 3: One parameter bifurcation diagram, for fixed $v_{ref} \in (A, B)$. Vertical axis is the duty cycle d , horizontal axis is k_s . PD is the period doubling bifurcation, CC is the corner collision bifurcation.

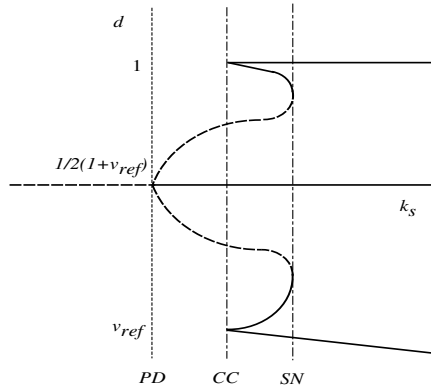


Figure 4: One parameter bifurcation diagram, for fixed $v_{ref} \in (B, C)$. Vertical axis is the duty cycle d , horizontal axis is k_s . PD is the period doubling bifurcation, CC is the corner collision bifurcation and SN is the saddle node bifurcation.

the period doubling at $k_s = 2.8483047$. At $k_s = 2.84826$, we found this stable solution with $d_1 = 0.99861$, $d_2 = 0.01139$ (solution eigenvalues are 0.883246 and 0.999996). There is also a range of values, between the period doubling and saddle node bifurcations, for which the stable T -periodic solution occurs at the same time as the unsaturated stable $2T$ -periodic solution. Thus for $v_{ref} = 0.01$ and $k_s = 2.84832$, that is to the right of the period doubling curve, we found an

unsaturated $2T$ -periodic solution with $d_1 = 0.9679, d_2 = 0.0421$. This solution was stable up to at least $k_s = 2.9$.

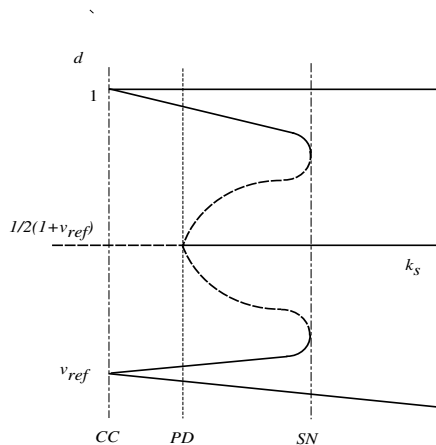


Figure 5: One parameter bifurcation diagram, for fixed $v_{ref} \in (C, F)$, for $v_{ref} > 0$. Vertical axis is the duty cycle d , horizontal axis is k_s . CC is the corner collision bifurcation, PD is the period doubling bifurcation and SN is the saddle node bifurcation.

8 Conclusions

We have proved a very useful result, lemma 3.1, for control problems with a strategy based on average quantities. In the case of the DC/DC buck converter with the ZAD strategy, this result allows us to calculate exactly the duty cycle d of a periodic system response, in the absence of detailed knowledge of the dynamics of the problem. We also calculated the period doubling bifurcation curve of a T -periodic response in the (v_{ref}, k_s) plane, given exact results for points on the curve in the limiting cases $v_{ref} = \pm 1$ and calculated the corner collision bifurcation curve where the $2T$ -periodic solution saturates. The period doubling and corner collision curves intersect tangentially at $v_{ref} = \pm 1$. We have discovered a codimension two bifurcation point where the corner collision curve collides with a saddle node bifurcation and also given different codimension one bifurcation diagrams that occur in this system as the duty cycle, d , varies with k_s for fixed v_{ref} .

Acknowledgements

The authors are very grateful to Fabiola Angulo, Mario di Bernardo and Gerard Olivar for extremely stimulating discussions. This work was partly funded by the EPSRC grant GR/72020/01, by European sponsored Project SICONOS, IST-2001-37172 and by the Spanish MCyT-FEDER grant BFM2003-09504-C02-02.

References

- [1] Angulo, F., Fossas, E. & Olivar, G. 2005 Transition from periodicity to chaos in a PWM-controlled buck converter with ZAD strategy. *Int. J. Bif. Chaos* **15**, 3245–3264.
- [2] Angulo, F., Di Bernardo, M., Hogan, S. J., Kowalczyk, P. & Olivar G. 2005 On two-parameter non-smooth bifurcations in power converters. In *IEEE International Symposium on Circuits and Systems, Kobe, Japan, 23-26 May*.
- [3] Angulo, F., Fossas, E. & Seara T. M. 2005 Applied perturbation theory to power converters regulation. Proceedings ENOC-2005.
- [4] Banerjee, S. & Verghese, G. C. 2001 *Nonlinear phenomena in power electronics: attractors, bifurcations, chaos, and nonlinear control*. New York: IEEE Press.
- [5] Biel D, Fossas E. & Griñó, R. 2001 Quasi-sliding control based on pulse width modulation, zero average and the L_2 norm. In *Advances in Variable Structure System, Analysis, Integration and Applications* (eds. X. Yu & J-X. Xu), pp. 335–344. Singapore: World Scientific.
- [6] Bilalovic, F., Music, O., & Sabanovic, A. 1983 Buck converter regulator operating in the sliding mode. In *Proceedings VII International PCI*. pp. 331–340.
- [7] Carpita, M., Marchesoni, M., Oberti, M. & Puguisi, L. 1988 Power conditioning system using slide mode control. In *Proceedings of the IEEE Power Electronics Specialist Conference*. pp. 623–633.
- [8] Di Bernardo, M., Budd, C.J., Champneys, A.R. & Kowalczyk, P. 2006 *Bifurcations in piecewise-smooth dynamical systems: theory and applications*, Springer-Verlag: Berlin
- [9] Fossas, E. & Olivar, G. 1996 Study of chaos in the buck converter. *IEEE Trans. Circ. Systems I* **43**, 13–25.
- [10] Fossas E. & Zinober A. 2001 Adaptive tracking control of nonlinear power converters. In *Proceedings IFAC Workshop on Adaptation in Control and Signal Processing. Connobio. Italy*. pp. 264–266.
- [11] Kowalczyk, P., Di Bernardo, M., Champneys, A.R., Hogan, S.J., Homer, M.E., Kuznetsov, Yu.A., Nordmark, A. & Piiroinen, P.T. 2006 Two-parameter discontinuity-induced bifurcations of limit cycles: classification and open problems. *Int. J. Bif. Chaos* **16**, 601–629.
- [12] Mohan, N., Undeland, T. M. & Robbins, W. P. 2002 *Power electronics: converters, applications, and design*. New York: Wiley.

- [13] Ramos, R., Biel, D., Fossas, E. & Guinjoan F. 2003 Fixed-frequency quasi-sliding control algorithm: application to power inverters design by means of FPGA implementation. *IEEE Trans. Power Electronics* **18**, 344–355.
- [14] Venkataramanan, R., Sabanović, A., & Čuk S. 1985 Sliding mode control of DC-to-DC converters. In *Proceedings IECON 1985*. pp. 251–258.
- [15] Yuan, G., Banerjee, S., Ott, E. & Yorke, J. A. 1998 Border-collision bifurcations in the buck converter. *IEEE Trans. Circ. Systems I* **45**, 707–716.